Transactions, SMiRT-24
BEXCO, Busan, Korea - August 20-25, 2017
Division SS

FAULT RUPTURE SIMULATION OF THE 2014 KAMISHIRO FAULT NAGANO PREFECTURE EARTHQUAKE USING 3D-FEM

Naoki Iwata[1], Ko Adachi[2], Yasunori Takahashi[2], Ömer Aydan[3], Takatoshi Ito[4] and Fusanori Miura[5]

[1] General Manager, Nuclear Project Department, Chuden Engineering Consultants Co., Ltd., Japan
[2] Nuclear Project Department, Chuden Engineering Consultants Co., Ltd., Japan
[3] Professor, Department of Civil Engineering, University of the Ryukyus, Japan
[4] Professor, Institute of Fluid Science, Tohoku University, Japan
[5] Professor, Science and Engineering, Yamaguchi University, Japan

ABSTRACT

As the 1999 Chi-chi earthquake and the 1999 Kocaeli earthquake damaged many important structures due to surface rupture as well as a strong motions induced by the earthquake faults, displacement and inclination of ground surface have become the significant issues in engineering. Most analytical methods do not evaluate displacement and strong motions at the same time. Iwata et al. (2016) conducted fault rupture simulation using three dimensional finite element method (3D-FEM) for the 2014 Nagano Prefecture Earthquake caused by the rupture of Kamishiro Fault. While the surface displacement response was in good agreement with the actual displacement, the acceleration response was not well simulated due to FEM mesh size, constitutive relation of fault plane and so on.

In this study, the authors revised simulation conditions such as damping ratio, spring stiffness of joint elements, FEM mesh size of a fault plane and the constitutive relation during stress drop to evaluate the acceleration response together with the consideration of the surface rupture. The computational results confirmed that the displacement and strong motion can be evaluated simultaneously using appropriate constitutive parameters and fine FEM mesh with a size less than 150m.

INTRODUCTION

The 1999 Chi-chi earthquake and the 1999 Kocaeli earthquake damaged many important structures due to surface rupture as well as high strong motions induced by the earthquake faults, which indicated the significance of displacement and inclination of ground surface on the response and damage of structures. Generally strong motions are estimated by Green's function method and fault displacement is estimated from geological surveys. However an earthquake occurs by rupture of earthquake source fault. When the displacement is large, it will reach the ground surface and appear as a surface rupture. Therefore, ideal analytical model should be able to simulate a fault rupture process and estimate displacement and strong motion at the same time. Fault rupture simulations by Finite Difference Method (FDM), Finite Element Method (FEM) and Boundary Element Method (BEM) are generally carried out. However, they have not become practical as analytical results greatly vary according to assumed initial stress conditions and modelling of fault rupture.

In the past study, Iwata et al. (2016) conducted fault rupture simulation using three dimensional finite element method (3D-FEM) for the 2014 Kamishiro Fault Nagano Prefecture Earthquake (M_w6.3), which is a thrust fault type earthquake with an observed surface rupture of 9km in length. A finite element model incorporating the fault rupture process proposed by Toki and Miura (1985) and Toki and Sawada (1988) was used to simulate the 2014 Nagano-Hokubu earthquake and its induced ground motions. Although the surface displacement response was in good agreement with the actual displacement, the

acceleration response was not well simulated due to FEM mesh size, constitutive relation of fault plane and so on.

In this study, we carried out a series of numerical analyses on fault rupture simulation under various conditions to investigate the influence of damping ratio, spring stiffness of joint element, variation of FEM mesh size of a fault plane and the constitutive relation during stress drop. Validity of parameters and modelling was evaluated by comparison with the observed surface ground motions recorded at K-NET Hakuba station located approximately 0.5km away from surface rupture.

OUTLINE OF ANALYTICAL METHOD

If the equation of motion involves the rupture movement of fault plane, it is necessary to treat the motion as a nonlinear problem. Therefore, it is appropriate to obtain a solution for the equation of motion not in frequency domain but rather in the time domain. The destruction process of dislocation and the dynamic behavior of ground are calculated by solving the equation of motion using stress drop of dislocation as external force. The equation of motion at time step n is written as;

$$[M]\{\ddot{u}\}_n + [C]\{\dot{u}\}_n + [K]\{u\}_n = \{F(n,s)\} \tag{1}$$

where $[M]$ is mass matrix, $[C]$ is damping matrix, $[K]$ is stiffness matrix, $\{\ddot{u}\}$ is acceleration vector, $\{\dot{u}\}$ is velocity, $\{u\}$ is displacement and $\{F(n,s)\}$ is the external force vector calculated from the dynamic stress drop ; n and s stand for time step and nodal pairs where fault rupture takes place, respectively. The damping matrix $[C]$ is obtained from the linear combination of $[M]$ and $[K]$, which is called Rayleigh damping, and is expressed as follows:

$$[C] = \alpha[M] + \beta[K] \tag{2}$$

$$\alpha = 2f_1 f_2 \frac{h_1 f_2 - h_2 f_1}{f_2^{\,2} - f_1^{\,2}}, \quad \beta = 2\left(\frac{h_2 f_2 - h_1 f_1}{f_2^{\,2} - f_1^{\,2}}\right) \tag{3}$$

where α and β are coefficients calculated by Eq.(3), f_1 and f_2 are frequency at the first and second modes, h_1 and h_2 are damping ratios at the first and second modes. Eq.(1) is solved using the Newmark's β method, β=0.25, γ=0.5, at each time interval. To solve the nonlinear equation of motion, we employed the load transfer method utilizing initial stiffness method (Toki and Miura, 1985, Toki and Sawada, 1988).

The fault plane is modelled by joint elements shown in Figure 1(a). The shear springs K_s, K_r and normal spring K_n are connections between nodal points of solid elements and a sliding obeys to Mohr-Coulomb failure criterion. Strength of Mohr-Coulomb failure criterion is generally estimated using cohesion and friction angle. However, friction angle is assumed to be zero as normal stress acting on fault plane is not known. The constitutive relation that represents the relation between the shear stress and

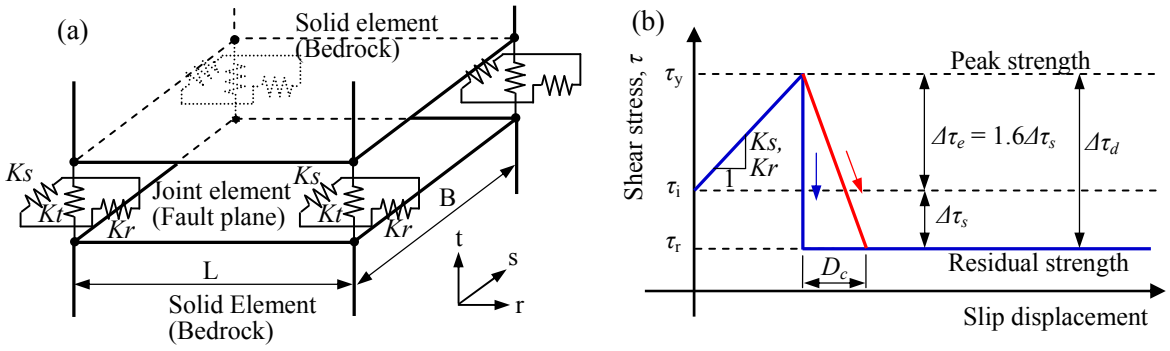

Figure 1. Three-dimensional joint element: (a) Schematic diagram of joint element in 3D-FEM, (b) Constitutive relation of joint element.

deformation is shown in Figure 1(b). When the shear stress τ is less than the peak stress τ_y, the stress-deformation relation is linear with the joint stiffnesses K_s, K_r. Sliding takes place if the shear stress τ reaches the peak stress τ_y and stress drop occurs. The shear stress becomes equivalent the residual strength τ_r and stress drop $\Delta\tau_d$ (= τ_y - τ_r) is released and transferred to nearby elements. In this way, the released stress drop in the hypocenter is triggered, shear failure propagates to surrounding areas with increasing of shear stress. In the past study, the peak stress instantly becomes the residual strength, however, the peak stress in the slip-weakening behaviour based on laboratory experiments exponentially decreases with the increase of relative displacement (Ohnaka and Yamashita, 1989). In this study, relationship between stress drop, $\Delta\tau_d$, and critical slip displacement, D_c, is assumed linear as shown in Figure 1(b).

OVERVIEW OF THE 2014 KAMISHIRO FAULT NAGANO PREFECTURE EARTHQUAKE

The 2014 Kamishiro Fault Nagano Prefecture Earthquake Japan, with a moment magnitude of 6.3, occurred at 22:08 JST on November 22 at northern part of Nagano Prefecture. Figure 2 shows schematic diagram of the fault plane. The fault plane is 15km long and 15km wide and the focal depth is estimated to be 5-6km (F-net, 2014, ERI, 2014 and JMA, 2014). The slip sense is estimated to be thrust faulting with left-lateral strike slip in N16E-50E and rake angle of 50 degrees (F-net, 2014 and ERI, 2014). The surface rupture appeared at southern 9km of the fault and the average dislocation in fault plane was 80cm.

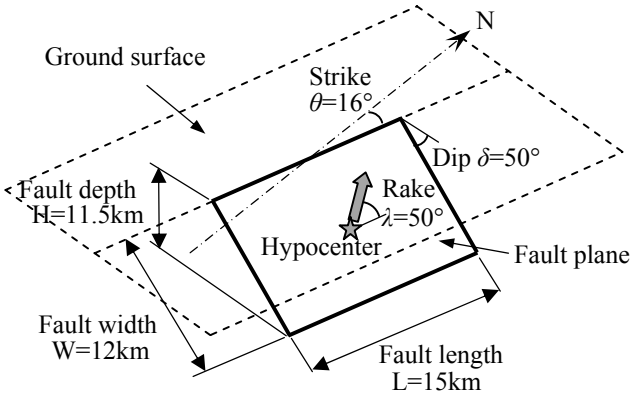

Figure 2. Schematic diagram of the fault plane

Figure 3 shows acceleration records at K-NET Hakuba station, which is one of the strong motion stations of the dense strong motion network operated by NIED and located approximately 0.5km away from surface rupture in the west. The maximum accelerations was 570Gal horizontally and 278 Gal vertically. The displacement response shown in Figure 3(a) was calculated using the EPS method proposed by Aydan and Ohta (2011), which is an integration technique to obtain ground motions with the consideration of device operation features, fault rupture duration and arrival time difference of P-wave and S-wave. From these results, residual displacement was obtained as 24cm horizontally and 10cm vertically. As shown in Figure 3(b), the spectrum in N-S direction is larger than that in E-W direction for whole periods, and the predominant period in N-S and E-W direction are around 0.2-0.3s, 0.1-0.3s respectively and the predominant period in N-S direction is slightly larger than that in E-W direction. The predominant period in U-D direction is less than 0.1s and shorter than that in horizontal direction.

ANALYTICAL CONDITIONS AND PARAMETERS

To investigate the influence of damping ratio, spring stiffness of joint element, the division size of FEM mesh of a fault plane, critical slip displacement during stress drop, we performed a series of fault rupture

simulations under various conditions as given in Table 1. Young's modulus and Poisson's ratio are determined by P-wave and S-wave. The average static stress drop $\Delta\tau_s$ in the fault plane is calculated from seismic moment and fault area (Sato, 1989). The peak strength τ_y is determined based on knowledge that excess strength $\Delta\tau_e$ is 1.6 times of the static stress drop $\Delta\tau_s$ (Andrew, 1987) and the residual strength τ_r made 10.0MPa larger enough than dynamic stress drop $\Delta\tau_d$. The first and second frequencies for Rayleigh damping, f_1 and f_2, are determined so that the response spectrum is almost distributed between two determined frequencies and damping ratio for f_1 and f_2 are assumed to be the same. The shear stress of hypocenter is assumed to be slightly larger than the peak strength τ_y. The shear stress distribution on the fault plane is assumed to have a mountain shape and average static stress drop $\Delta\tau_s$ became 2.0 MPa (Fukushima et al., 2010).

Table 1: Geophysical parameters and geometric condition for numerical analysis

Bedrock	
Elastic velocity of S wave, V_S (m/s)	3,500
Elastic velocity of P wave, V_P (m/s)	6,100
Unit weight, γ_t (kN/m^3)	26.5
Poisson's ratio, ν	0.25
Fault	
Shear stiffness, K_s (GN/m^3)	10, 1, 0.1, 0.01
Normal stiffness, K_n (GN/m^3)	$3\times K_s$
Static stress drop, $\Delta\tau_s$ (MPa)	2.0
Peak strength, τ_y (MPa)	15.2
Residual strength, τ_r (MPa)	10.0
Critical slip displacement, D_c (m)	0.0, 0.01, 0.05, 0.1.0.2
Rayleigh damping	
Damping ratio, h	0.01, 0.03, 0.05, 0.1
Frequency, f (Hz)	f_1=0.05, f_2=20
Division size FEM mesh of a fault plane, B (m)	500, 300, 200, 150

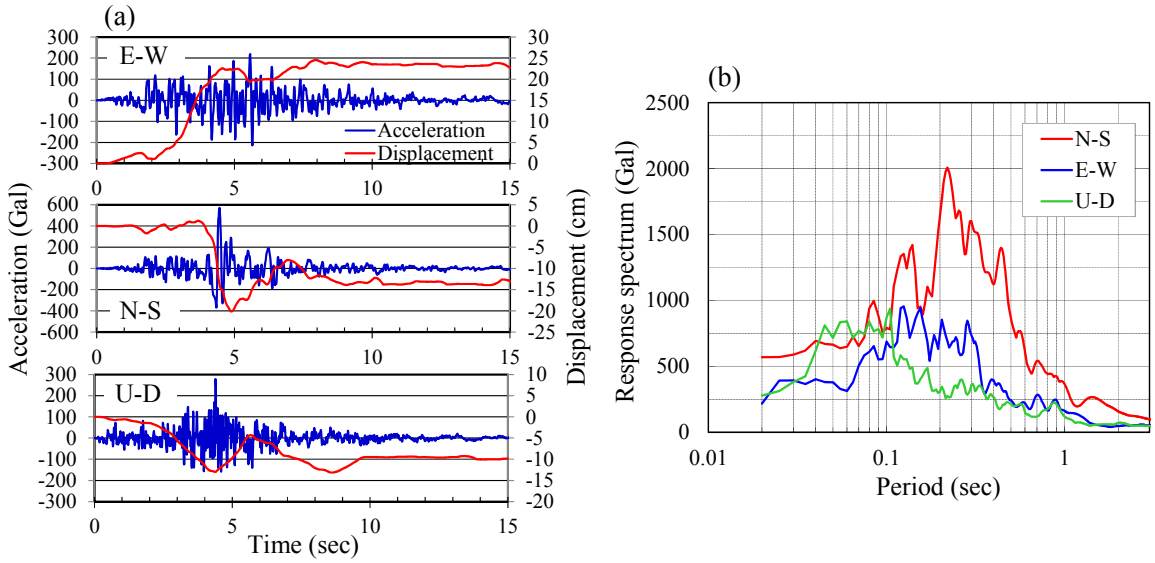

Figure 3. Acceleration records at K-NET Hakuba station and displacement time histories calculated by the EPS method.

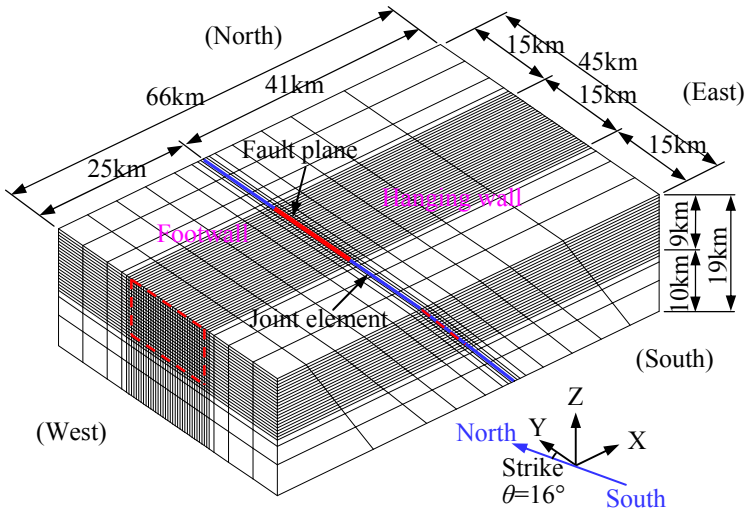

Figure 4. 3D FEM mesh

Figure 4 shows 3D-FEM model that the fault plane is divided into 500m. Joint elements are set up from north lateral boundary to south one and the strength of joint elements located in out of the fault plane is set to have larger value. The distance from the fault edge to the boundaries is more than fault length (15km) and the viscous dampers were introduced at the lateral and bottom boundaries to absorb scattering wave energy.

ANALYTICAL RESULTS

Influence of damping ratio

We conducted fault rupture simulation using different damping ratio: h=0.01, 0.03, 0.05, 0.10. Other parameters are set as follows: the spring stiffness of joint element is 1 GN/m^3, FEM mesh size of a fault plane is 500m and critical slip displacement is zero; peak stress is dropped instantly to residual strength.

Figure 5 shows a comparison of analyzed acceleration waves at distances of 0.5km west from the surface rupture. The amplitude of acceleration wave becomes smaller as damping ratio increases, and the response after 4 seconds becomes smaller. Similarly, the analyzed displacement at the monitoring point becomes smaller as damping ratio increases.

Figure 6(a) shows the distributions of shear failure propagation time of the fault plane in the case of damping ratio : h=0.03. The rupture front spreads elliptically having the major axial direction along the slip direction and reaches the ground surface of fault center in 1.48 seconds and the lateral edges in 2.3-3.2 seconds. The rupture velocity from hypocentre to surface is 3.5km/s, it's same as the elastic velocity of S wave. Figure 6(b) shows the time histories of shear stress of the fault plane elements, which is shown in Figure 6(a): hypocenter, F-1 and F2. The shear stress is reduced to the residual strength just as shear stress reaches the peak stress. Accordingly the shear stress at hypocentre becomes equal to the residual strength. The shear stress increases in the element, which is near to the hypocentre, and reaches the failure limit. After reaching the peak stress level, the increase and decrease of shear stress occurs with yielding of neighboring elements. The distributions of shear failure propagation time are almost constant with damping ratio. Therefore, as seen in Figure 5, the response acceleration waves after 4 seconds are caused by waves reflected at the lateral boundary and the resonance of the FEM model. When the damping ratio is set to 0.03-0.05, the analyzed acceleration waves after main shock become smaller and become closer to the observations.

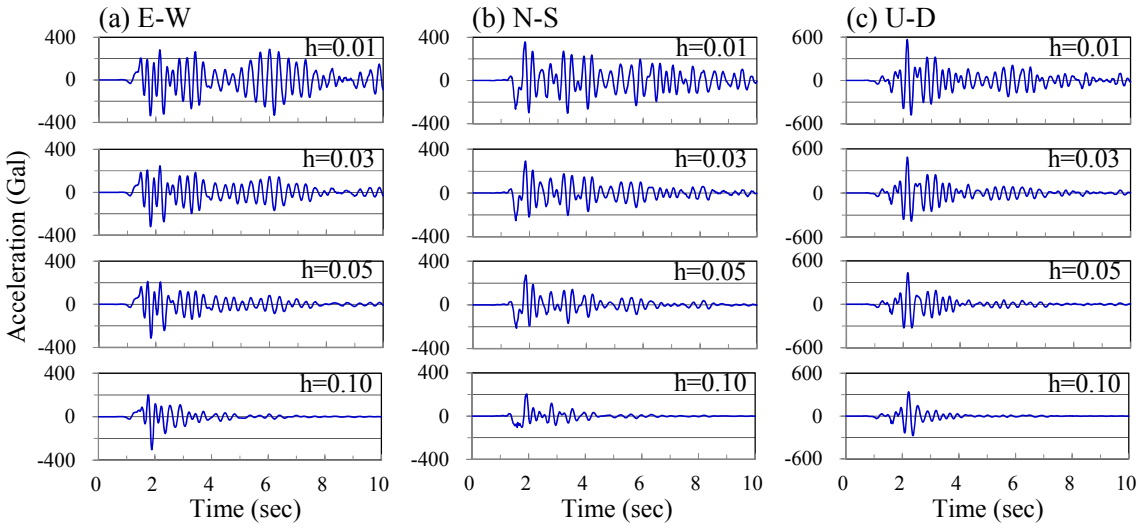

Figure 5. Comparison of analyzed acceleration waves at the ground surface in west 0.5km from the surface rupture using different Damping ratio: h=0.01, 0.03, 0.05, 0.10.

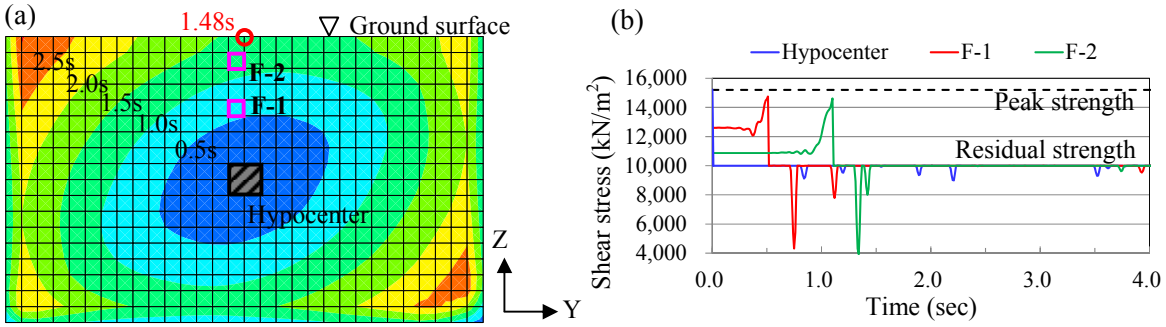

Figure 6. Rupture propagation on the fault plane in the case of damping ratio h=0.03: (a) Distributions of shear failure time, (b) Time histories of shear stress of the fault plane element.

Influence of spring stiffness of joint element

We carried out fault rupture simulations using different shear spring constants: K_s=10, 1, 0.1, 0.01GN/m^3. Other parameters are set as follows: the damping ratio is 0.03, FEM mesh size of a fault plane is 500m and critical slip displacement is zero.

Figure 7 compares analyzed acceleration waves at distances of 0.5km west from the surface rupture. The amplitude of acceleration wave in N-S direction becomes smaller as shear spring constant decreases and that in other directions become larger. However, in the case of shear spring constant, that is, K_s =0.01GN/m^3, the rupture does not propagate and only the neighbourhood of hypocenter is ruptured. If a shear spring constant is set smaller value, the shear stress of fault transferred from a yield element becomes smaller, and that of ground becomes larger. Therefore, the acceleration response in the fault plane direction, specifically, N-S direction, becomes smaller, and the acceleration response in a direction perpendicular to fault plane, specifically, E-W and U-D direction, which greatly influence ground shaking, becomes larger. In case of K_s=10, 1, 0.1GN/m3, the rupture front reaches the center of the fault trace at ground surface in 1.19, 1.48, 1.78 seconds, respectively. In case of K_s=10GN/m^3, the rupture velocity is 4.4 km/s. This result is not appropriate because the rupture velocity is larger than the elastic velocity of S wave: V_S=3.5km/s. Generally the rupture velocity is around 0.8 times of Vs (Somerville *et al*, 1999).

When joint elements are used for a contact surface, spring constant should be large as much as possible. The rupture velocity of K_s=1GN/m^3 is nearly equal to S wave velocity. Therefore, this value is used by the following calculation.

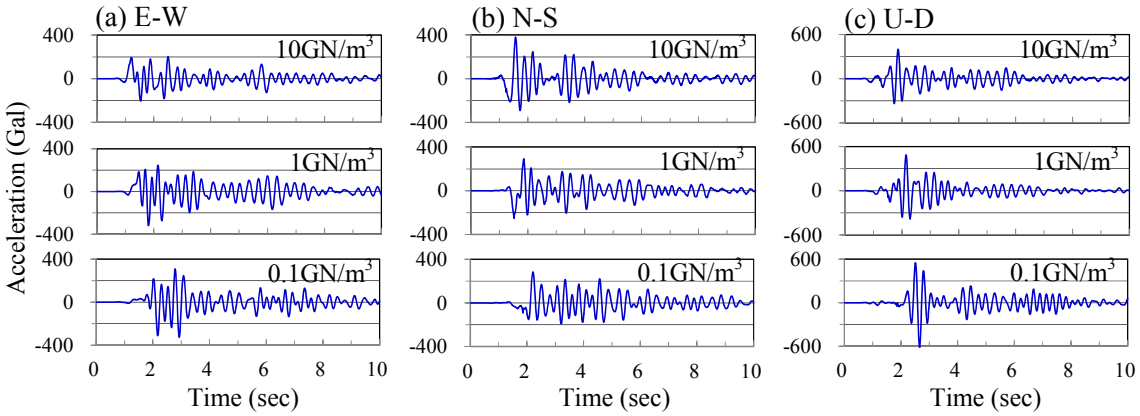

Figure 7. Comparison of analyzed acceleration waves at the ground surface in west 0.5km from the surface rupture using different shear spring constants: K_s=10, 1, 0.1, 0.01GPa/m.

Influence of FEM mesh size of fault plane

We performed fault rupture simulations using different FEM mesh size: B=500, 300, 200, 150m. Other parameters are set as follows: the damping ratio is 0.03, the spring stiffness of joint element is 1 GN/m^3 and critical slip displacement is zero.

Figure 8 shows comparison of analyzed acceleration waves at distances of 0.5km west from the surface rupture. When FEM mesh size becomes smaller, high frequency components of acceleration response increase and the response after main shock decreases because stress drop becomes small if FEM mesh size is small.

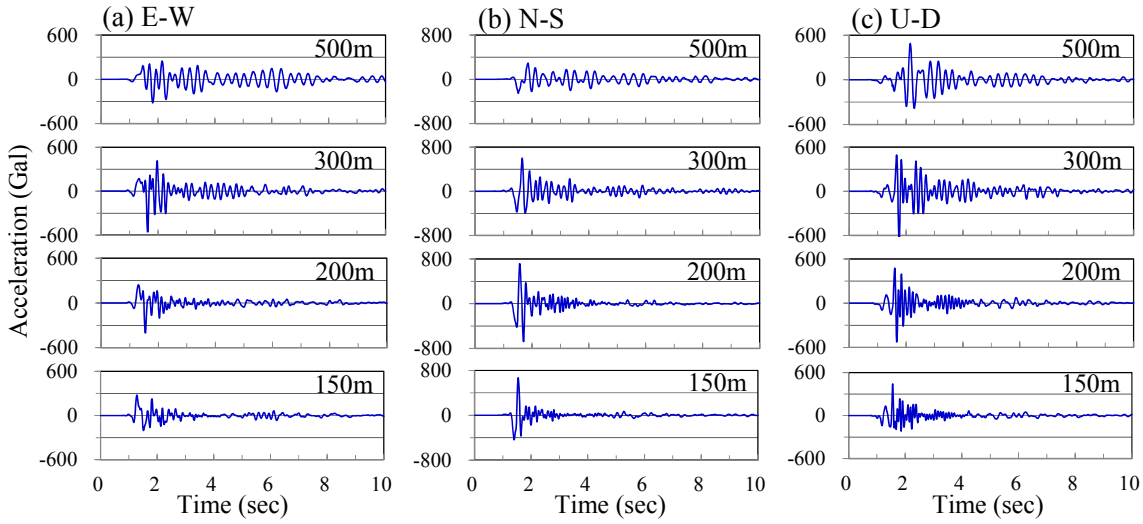

Figure 8. Comparison of analyzed acceleration waves at the ground surface in west 0.5km from the surface rupture using different FEM mesh size: 500, 300,200,150m.

Figure 9 shows comparison between response spectra at distances of 0.5km west from the surface rupture. Regarding the response spectra for E-W and U-D directions, the spectral peak shifts to the short period and becomes smaller as the FEM mesh size becomes smaller. As for response spectrum in N-S direction, the spectral peak slightly shifts to the short period and becomes larger. The response spectrum shape and peak value in E-W and N-S direction are closer to the observations if smaller mesh size is used. It is revealed that the response spectrum shape and peak value in horizontal direction can be simulated if mesh size is around 150m, and it is also necessary to assume smaller mesh size to simulate the motions in vertical direction.

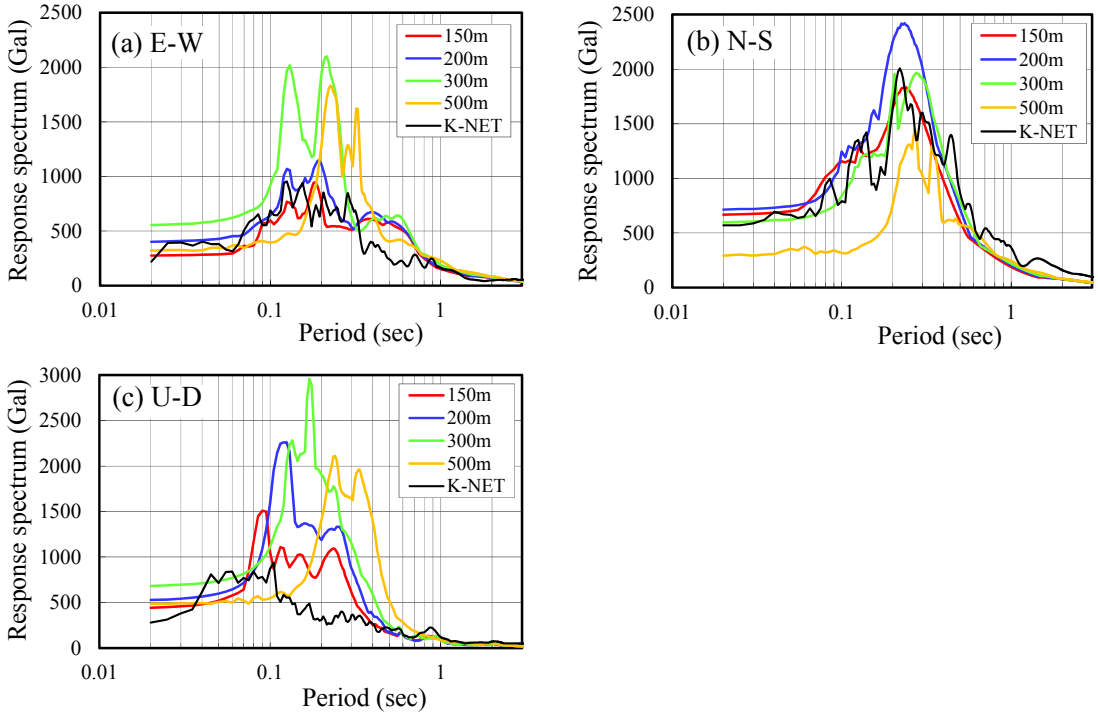

Figure 9. Comparison of acceleration response spectrum at the ground surface in west 0.5km from the surface rupture using different FEM mesh size: 500, 300,200,150m.

Influence of critical slip distance in stress drop

Fault rupture simulations were carried out using different critical slip displacement values: D_c=0.01, 0.05, 0.1, 0.2 m. Other parameters are set as follows: the damping ratio is 0.03, the spring stiffness of joint element is 1 GN/m^3 and FEM mesh size of a fault plane is 300m.

Figure 10 shows a comparison of analyzed acceleration waves at distances of 0.5 km west from the surface rupture using different critical slip distance : D_c=0.01, 0.05, 0.1 m. Furthermore, in the case of D_c=0.2 m, the rupture does not propagate and only the neighbourhood of hypocenter is ruptured. When critical slip distance becomes larger, the main shock is delayed and the amplitude of acceleration wave becomes smaller. The maximum acceleration occurs at around 2.8 seconds in case of D_c=0.1m. However, it is earlier than that of the observations.

Figure 11(a) shows the distributions of shear failure propagation time of the fault plane in the case of D_c =0.10m. The rupture front reaches the ground surface of fault center in 2.43 seconds and the lateral edges in 3.5- 4.5 seconds. The rupture velocity from hypocentre to surface is 2.1km/s. It is around 0.6 times of the elastic velocity of S wave and is slightly smaller than general rupture velocity. When critical slip distance is not considered, yielding spreads over the whole fault plane. To stop yielding, the strength

of joint elements located in out of fault plane is set large value. However, no destruction area remains in the bottom end of right and left when critical slip distance is considered. It implies that the spread of destruction could be stopped even if the destruction area of fault plane was not set previously using appropriate quantity of critical slip distance and stress drop. Figure 11(b) shows the time histories of shear stress of the fault plane element in the case of D_c =0.10m. Relation between slip distance and stress drop is linear as seen in Figure 2, although time variation of shear stress during stress drop is convex. It indicates sliding of fault increase moderately.

Figure 12 compares analyzed displacement response during rupturing. Similarly, the displacement is delayed as the slip distance is larger. However, the permanent displacement for all cases is almost the same. The analyzed residual displacement is in good agreement with the actual displacement.

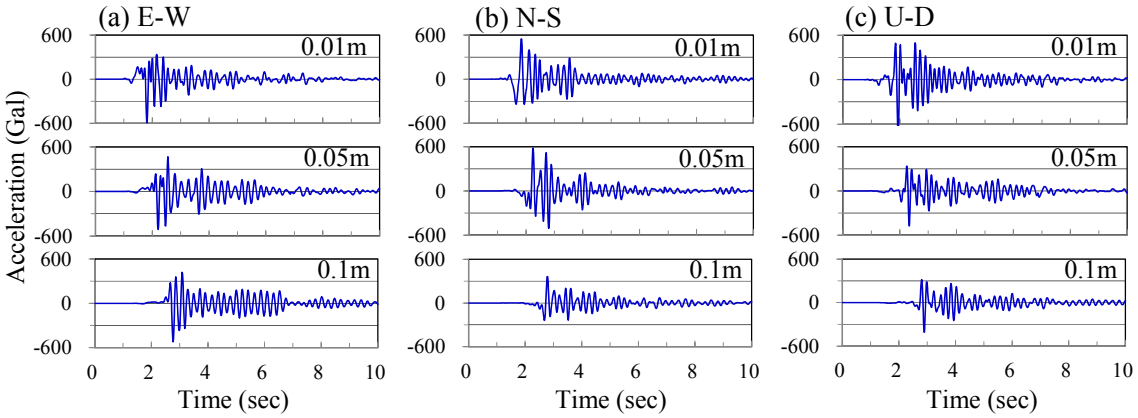

Figure 10. Comparison of analyzed acceleration waves at the ground surface in west 0.5km from the surface rupture using different critical slip distance : *Dc*=0.01, 0.05, 0.1m.

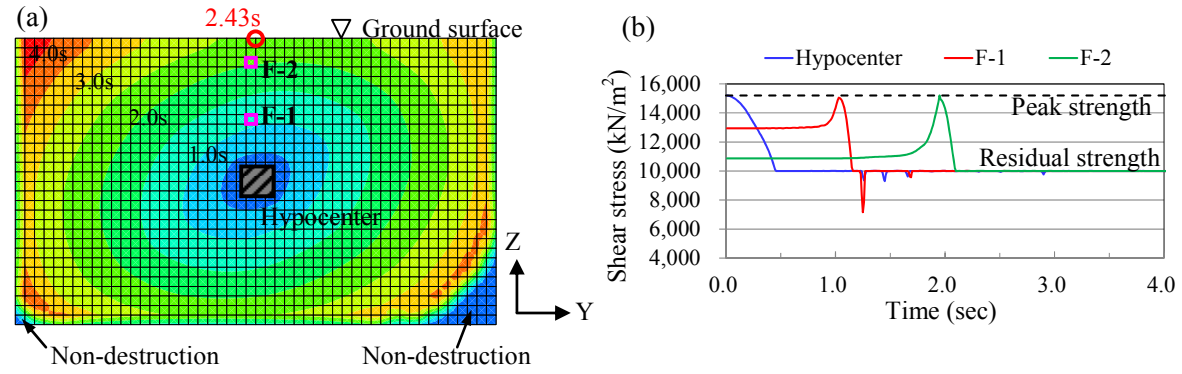

Figure 11. Rupture propagation on the fault plane in the case of D_c =0.10m: (a) Distributions of shear failure time, (b) Time histories of shear stress of the fault plane element.

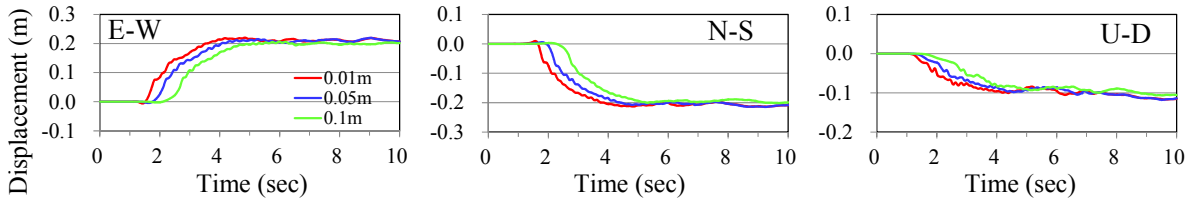

Figure 12. Comparison of analyzed displacement waves at the ground surface in west 0.5km from the surface rupture using different critical slip distance : D_c=0.01, 0.05, 0.1m.

CONCLUSIONS

In this study, we performed a series of fault rupture simulations using 3D-FEM for the 2014 Kamishiro Fault Nagano Prefecture Earthquake and evaluated the influences of FEM mesh and various conditions. The findings obtained from this study can be summarized as follows:

1. The horizontal acceleration is well simulated if a fault plane is discretized into small FEM mesh less than 150m. However, it is also necessary to discretize vertical direction into smaller finite elements in order to evaluate the vertical component of ground acceleration.
2. The peak acceleration and displacement are delayed as the shear spring constant becomes smaller and/or critical slip displacement becomes larger.
3. When the spring constant is less than 0.01GN/m^3 or critical slip displacement is more than 0.2m, the rupture does not propagate and only the neighbourhood of hypocenter is ruptured.
4. It is possible to simulate displacement and strong motion simultaneously using appropriate parameters and discretizing a fault plane into small FEM mesh less than 150 m.

We continue to simulate other earthquakes and examine the validity and the applicability of numerical method and modelling of a fault presented in this paper.

REFERENCES

Andrews, D.J. (1976). "Rupture velocity of plane strain shear cracks," *J. of Geo. Res.*, Vol. 81, No. 32, 5679-5687.

Aydan, Ö. and Ohta, Y. (2011). "The erratic pattern screening (EPS) method for estimation of co-seismic deformation of ground from acceleration records and its application", *Seventh National Conf. on Earth. Eng.*, Turkey.

ERI (Earthquake Research Institute, University of Tokyo). (2014). "Report of North Nagano Earthquake on November 22, 2014" (in Japanese).

F-net (Full Range Seismograph Network of Japan). (2014). "Topics: Earthquake in North Nagano on November 22, 2014" (in Japanese).

Fukushima, K., Kanaori, Y. and Miura, F. (2010). "Influence of fault process zone on ground shaking of inland earthquakes: verification of Mj=7.3 Western Tottori Prefecture and Mj=7.0 West Off Fukuoka Prefecture earthquakes," southwest Japan, *Eng. Geo.,* 116, 157-165.

Iwata, N., Adachi, K., Takahashi, Y., Aydan, Ö., Tokashiki, N. and Miura, F. (2016) "Fault rupture simulation of the 2014 Kamishiro Fault Nagano Prefecture Earthquake using 2D and 3D-FEM," *Proc*., *EUROCK 2016*, *Turkey*, 803-808.

JMA (Japan Meteorological Agency). (2014). "News release document about the earthquake of North Nagano on November 22, 2014 about 22:08" (in Japanese).

Ohnaka, M. and Yamashita, T. (1989) "A cohesive zone model for dynamic shear faulting based on experimentally inferred constitutive relation and strong motion source parameters," *J. Geophys*. *Res*., 94, 4089-4104.

Sato, R. (1989). "Japanese seismic dislocation parameter handbook, *Kashima Publication Society*," 309 (in Japanese).

Somerville, P.G., Irikura, K., Graves, R., Sawada, S., Wald, D., Abrahamson, N., Iwasaki, Y., Kagawa, T., Smith, N. and Kowada, A. (1999) "Characterizing crustal earthquake slip models for the prediction of strong ground motion," *Seismological Research Letters*, 70, 59-80.

Toki, K. and Miura, F. (1985). "Simulation of a fault rupture mechanism by a two-dimensional finite element method," *J. Phys. Earth.*, Vol. 33, 485-511.

Toki, K. and Sawada, S. (1988). "Simulation of the fault rupture process and near filed ground motion by the three-dimensional finite element method," *Proc., 9th World Conf. on Earth. Eng., Japan*, Vol. II, 751-756.